

**Ligand-regulated to prepare Fe,N,S tri-codoped hollow carbon
electrocatalyst for enhanced ORR performance and Zn-Air battery**

Yi Wu^a, Yvting Yang^b, Taotao Gao^b, Xiaojuan Chen^b, Zhihan Huang^b, Jinmei Zhang^a, Yong Guo^{*a}, Dan Xiao^{*ab}

^a College of Chemistry Sichuan University Chengdu, 610065, P.R.China

^b College of Chemical Engineering Sichuan University Chengdu, 610065, P. R. China

E-mail: guoy@scu.edu.cn, xiaodan@scu.edu.cn

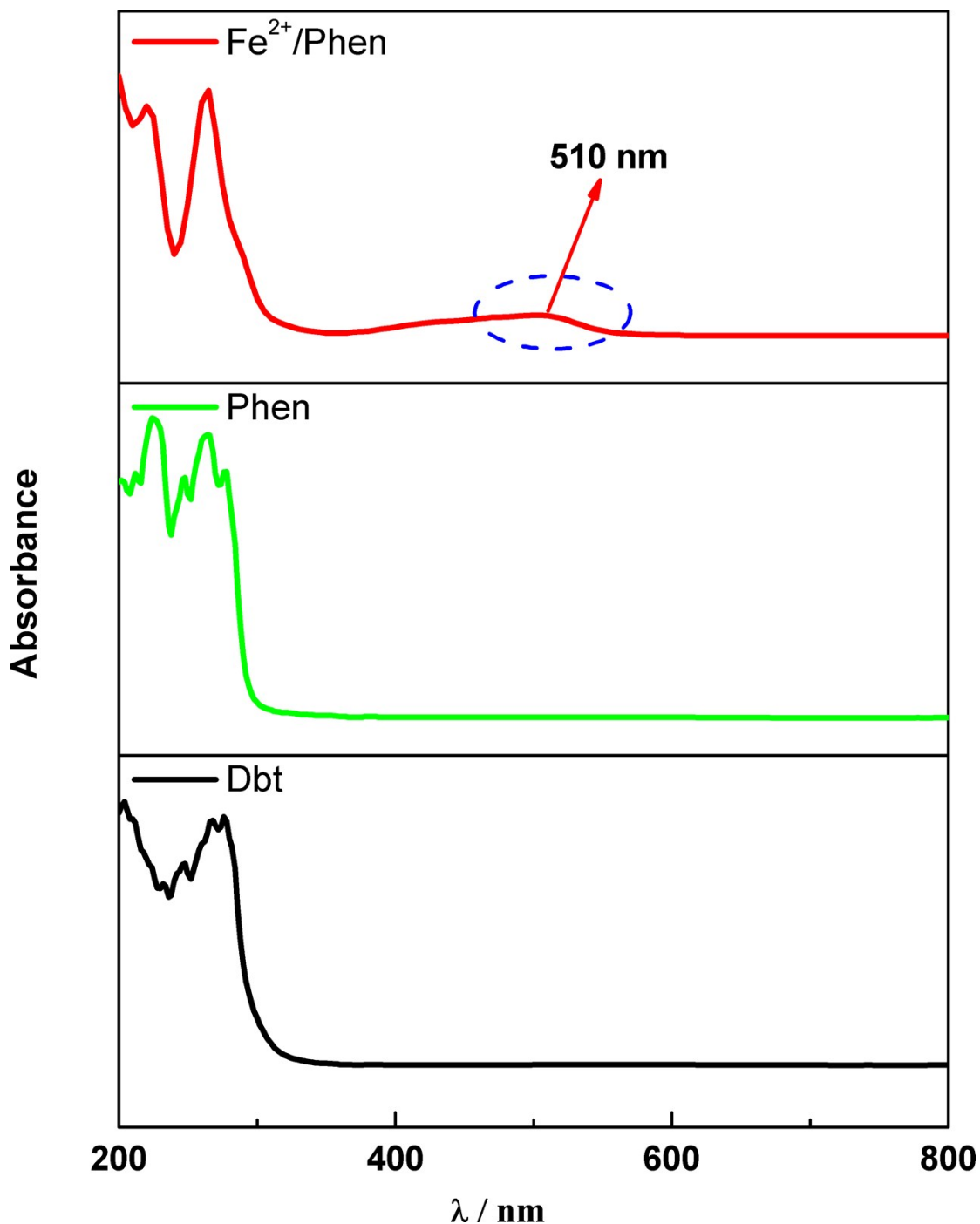


Fig. S1 UV-vis spectra for the $\text{Fe}^{2+}/\text{Phen}$ complex (solid red curve), phen ligand (solid green curve) and Dbt (solid dark curve) measured in ethanol solution.

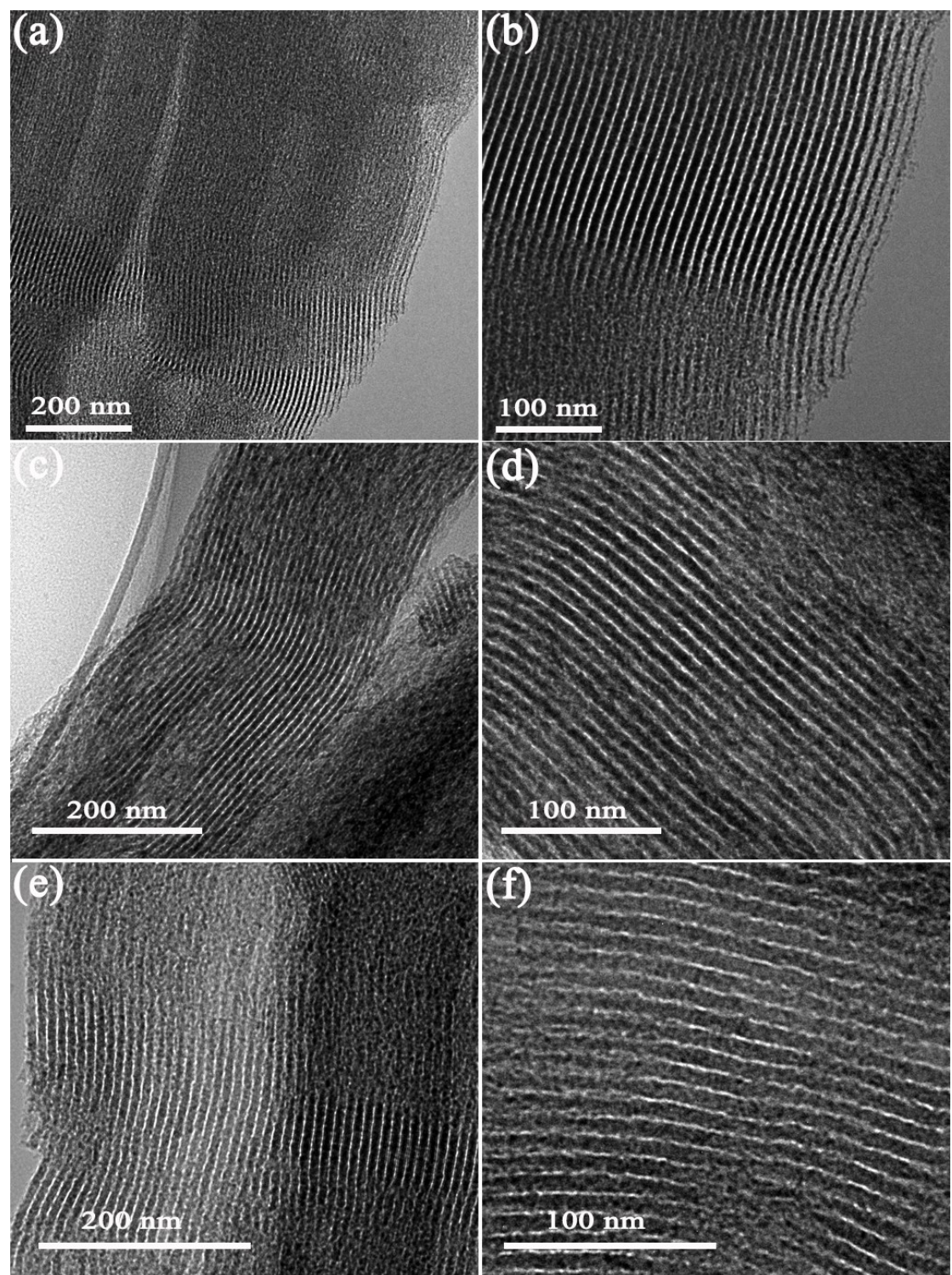


Fig. S2 (a,b) The TEM images of the SBA-15 template. (c,d) The TEM images of the Z-CNS-Fe-Dcb. (e,f) The TEM images of the Z-CNS-Fe-Bpd.

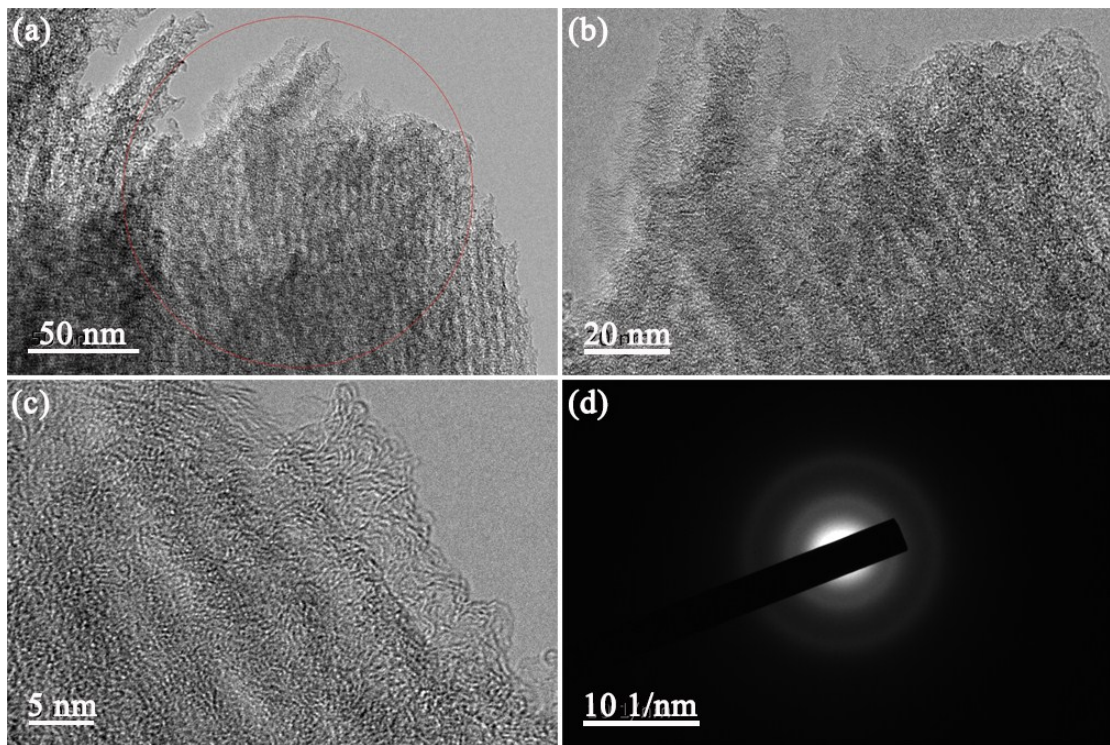


Fig. S3 (a-c) The different resolution HRTEM images and (d) the Selected area electron diffraction (SAED) pattern of Z-CNS-Fe.

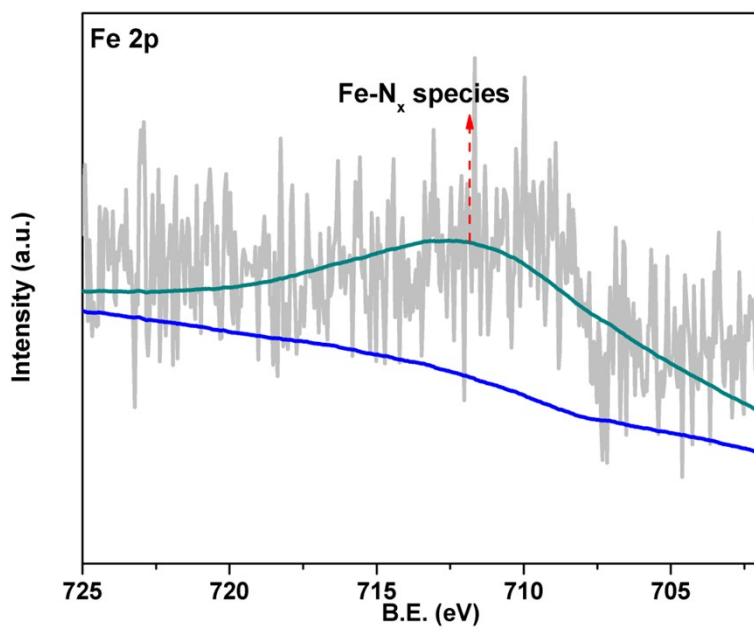


Fig. S4 Fe 2p XPS spectra of Z-CNS-Fe.

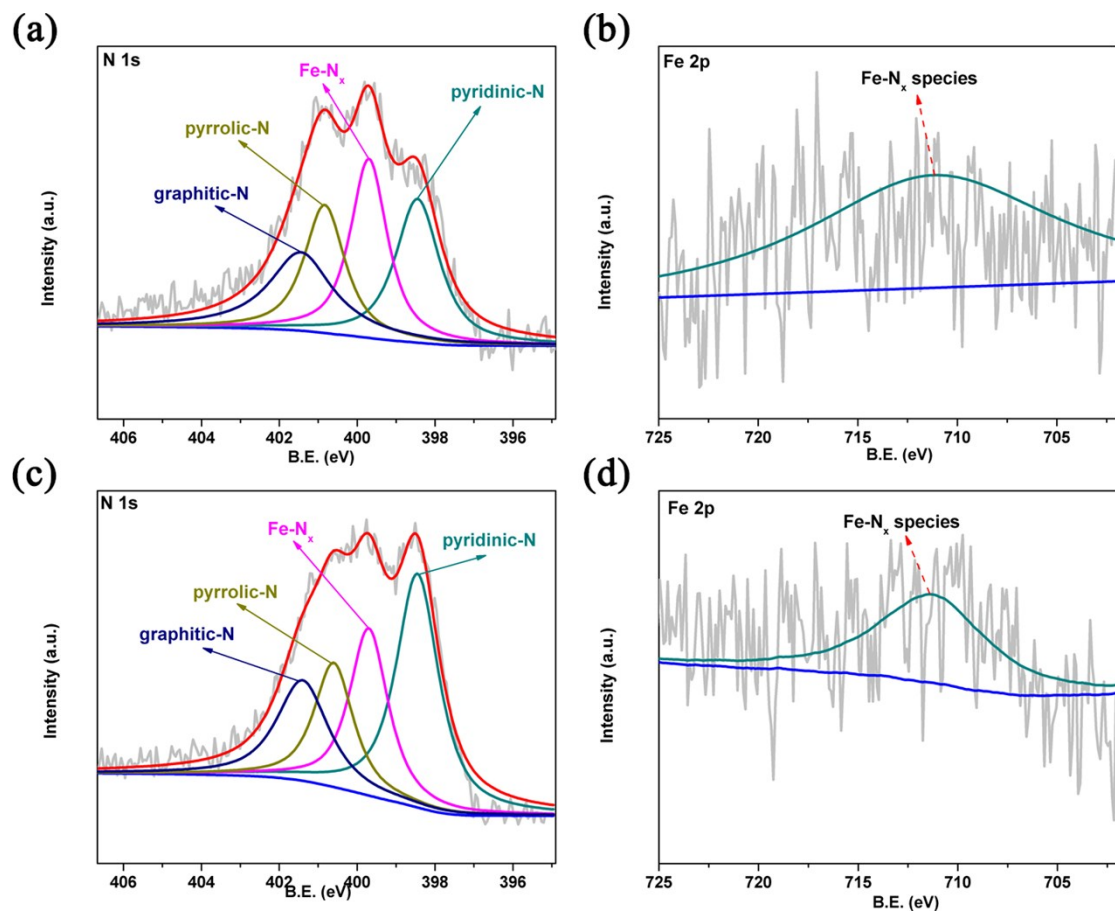


Fig. S5 (a,c) The high-resolution N 1s XPS spectra of Z-CNS-Fe-Dcb and Z-CNS-Fe-Bpd. (b,d) The high-resolution Fe 2p XPS spectra of Z-CNS-Fe-Dcb and Z-CNS-Fe-Bpd.

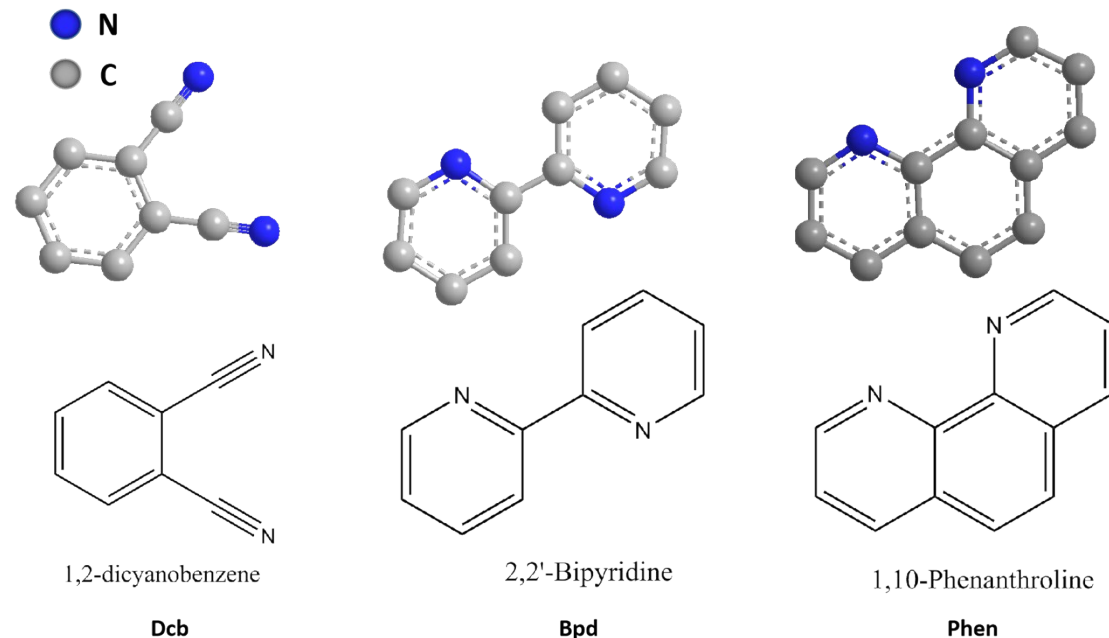


Fig. S6 The structural formula and ball-and-stick model of three different ligands.

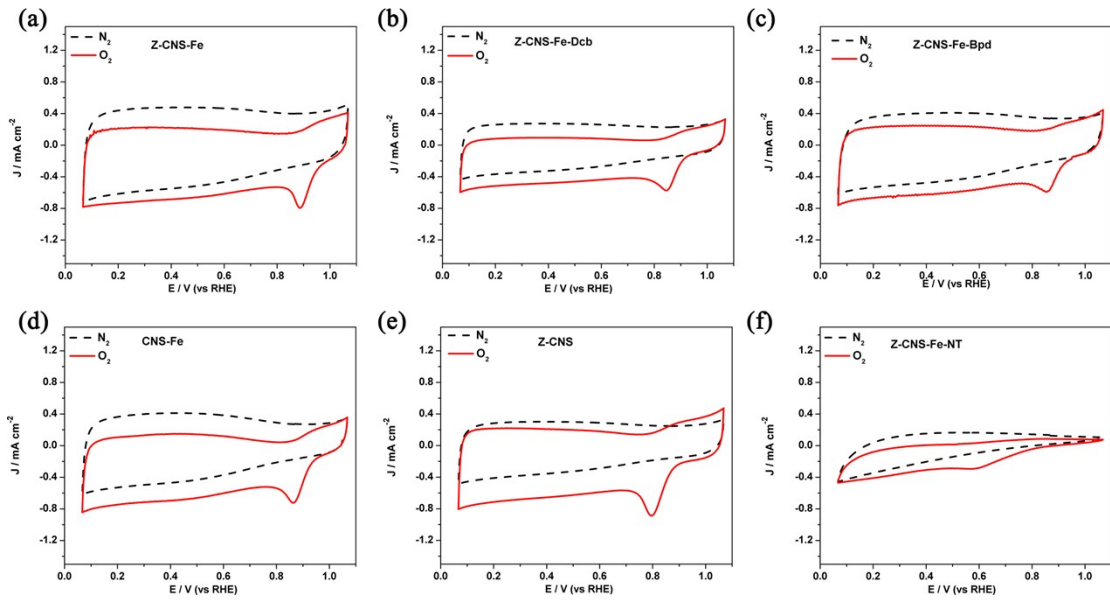


Fig. S7 The CV curves of the catalysts in N_2 (dashed black line) and O_2 (solid red line)-saturated 0.1 M KOH solution at the scan rate of 10 mV s^{-1} .

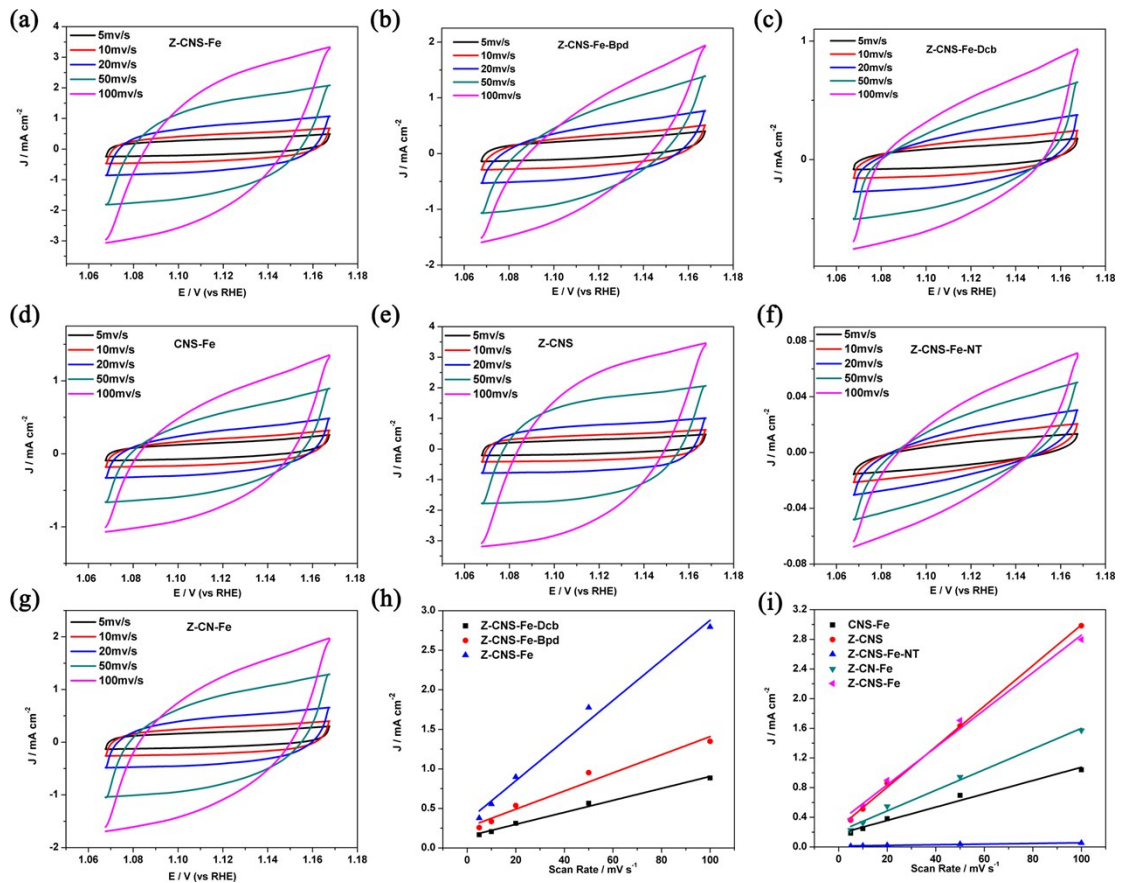


Fig. S8 (a-g) Capacitive CV profile recorded in non-Faradaic region with scan rates of 5, 10, 20, 50, 100 mV s^{-1} in 0.1 M KOH solution. (h-i) Current density (mA cm^{-2}) vs scan rates (mV s^{-1}) obtained from capacitive CV profile at potential of 1.14 V vs RHE of catalysts.

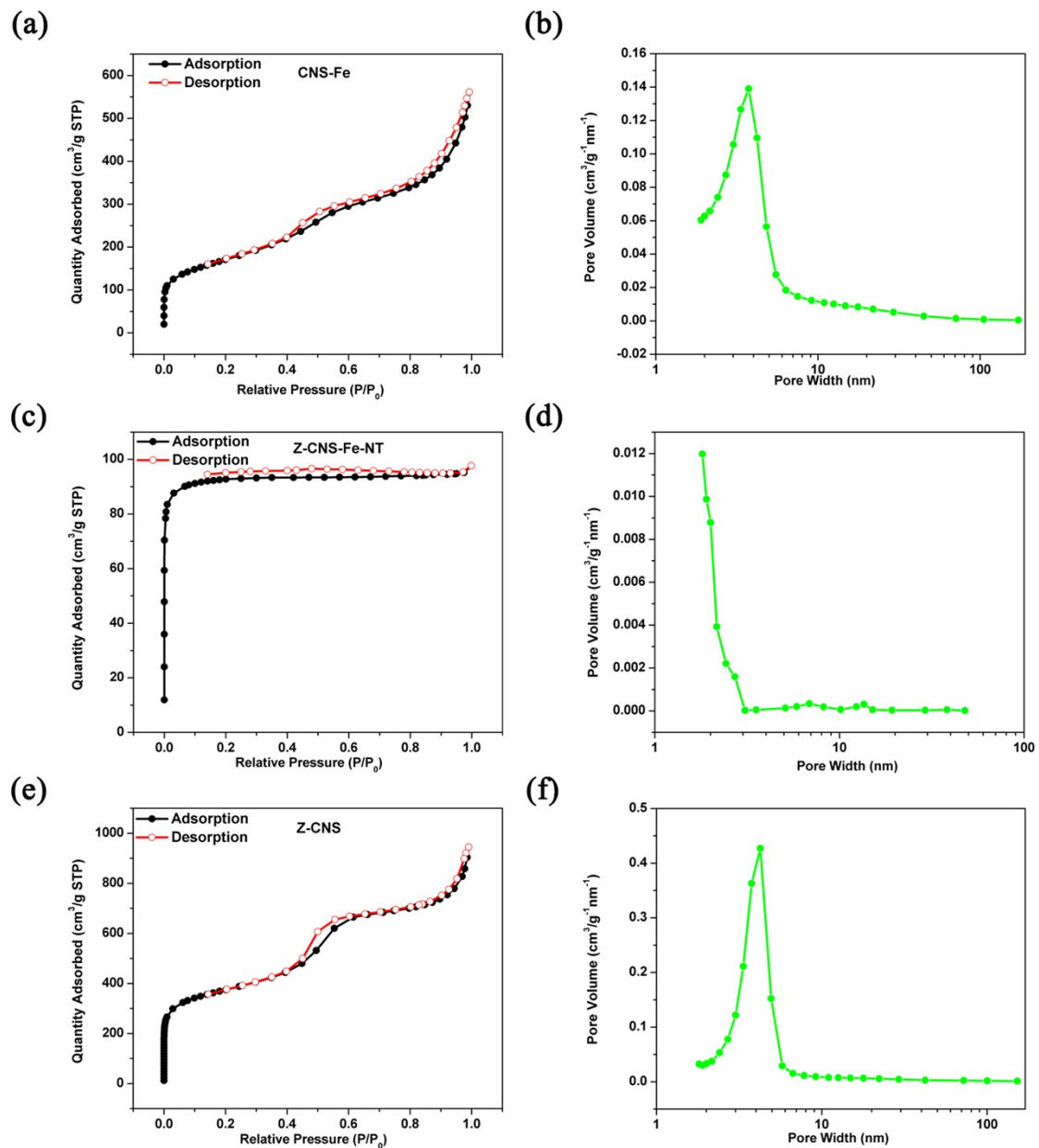


Fig. S9 (a-f) Nitrogen adsorption–desorption isotherm and pore size distribution of CNS-Fe, Z-CNS-Fe-NT and Z-CNS.

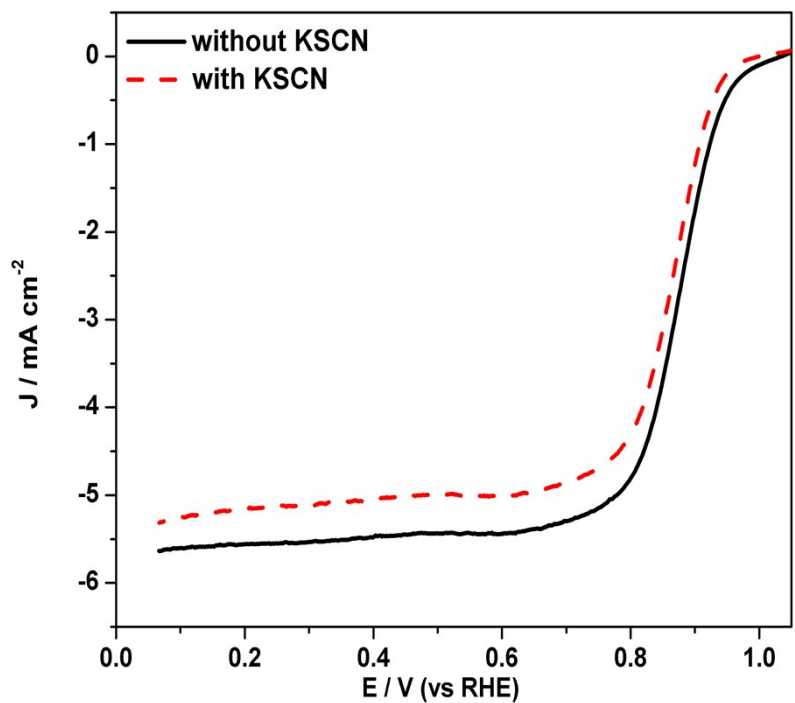


Fig. S10 The ORR LSV curves of Z-CNS-Fe before (solid black line) and after (dashed red line) the introduction of KSCN.

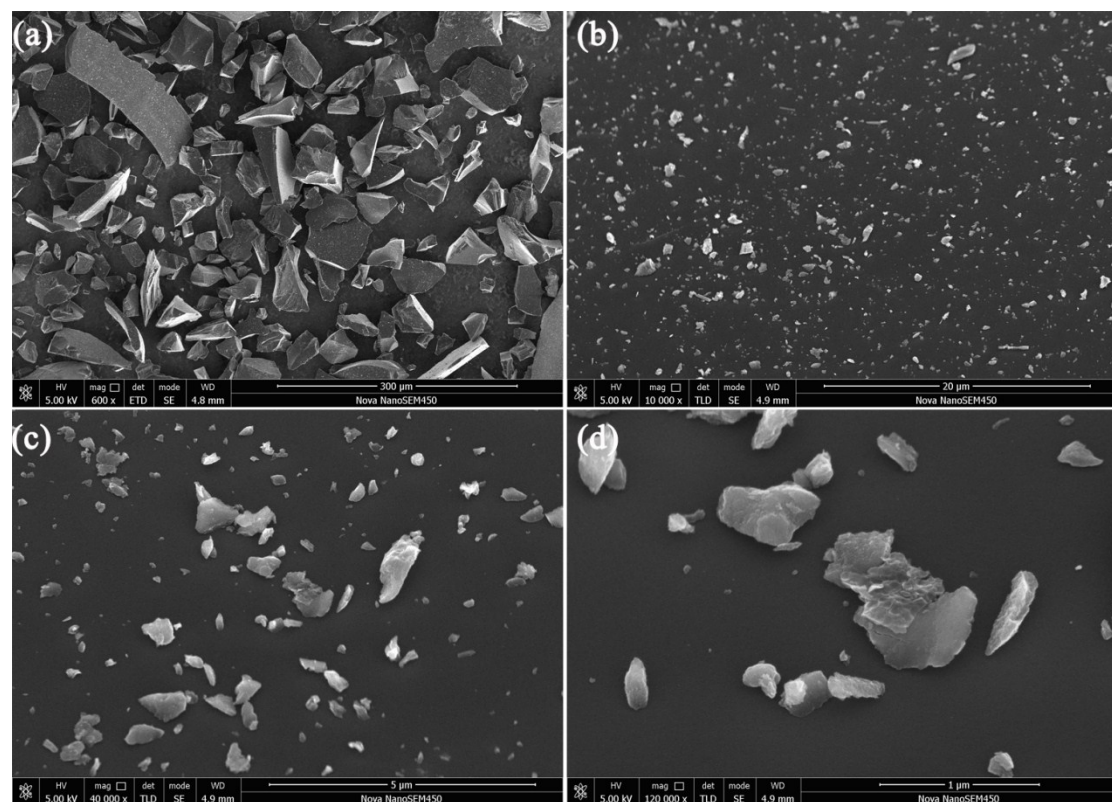


Fig. S11 The SEM images of the as-prepared Z-CNS-Fe-NT (a,b,c,d).

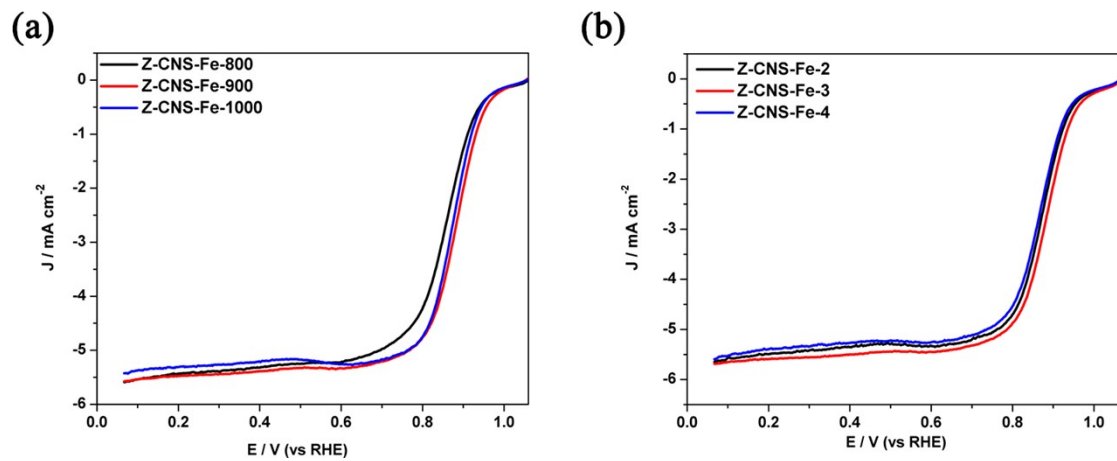


Fig. S12 (a-b) The ORR LSV plots of Z-CNS-Fe catalysts annealed with different temperatures, metal molar ratio in O_2 -saturated 0.1 M KOH solution at the speed of 1600 rpm.

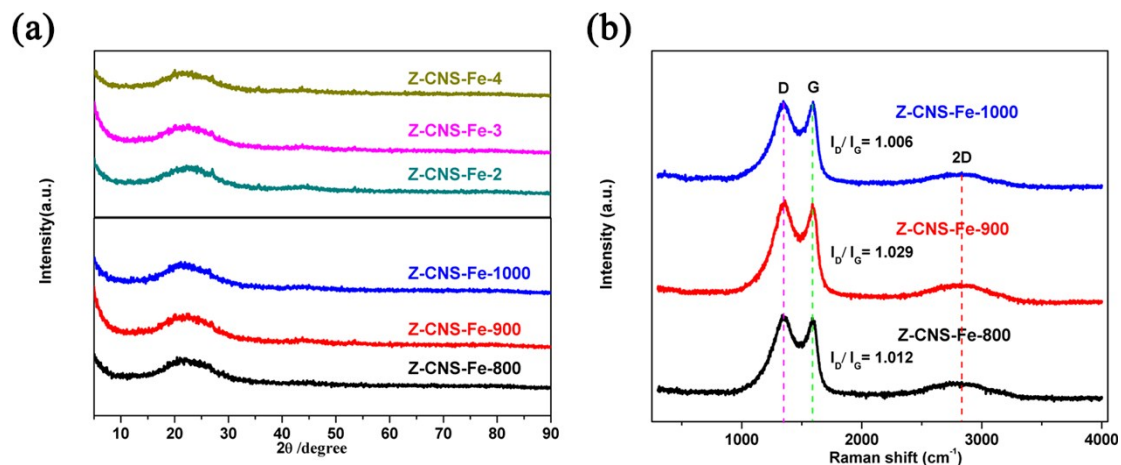


Fig. S13 (a) the XRD patterns of Z-CNS-Fe at different sintering temperature, metal molar ratio. (b) the Raman spectra of Z-CNS-Fe catalysts annealed with different temperatures.

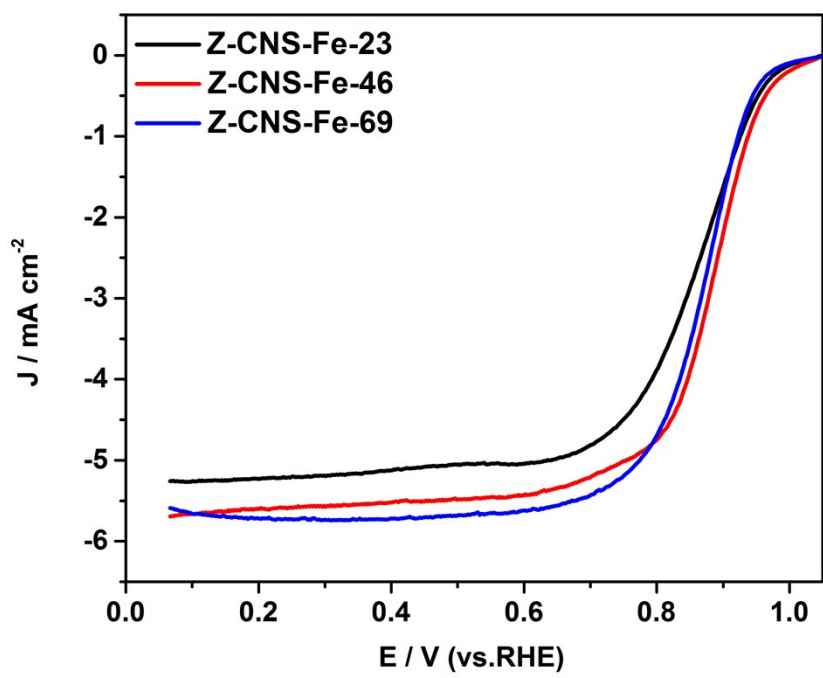


Fig. S14 The LSV curves of the materials made from different FeCl_2 content.

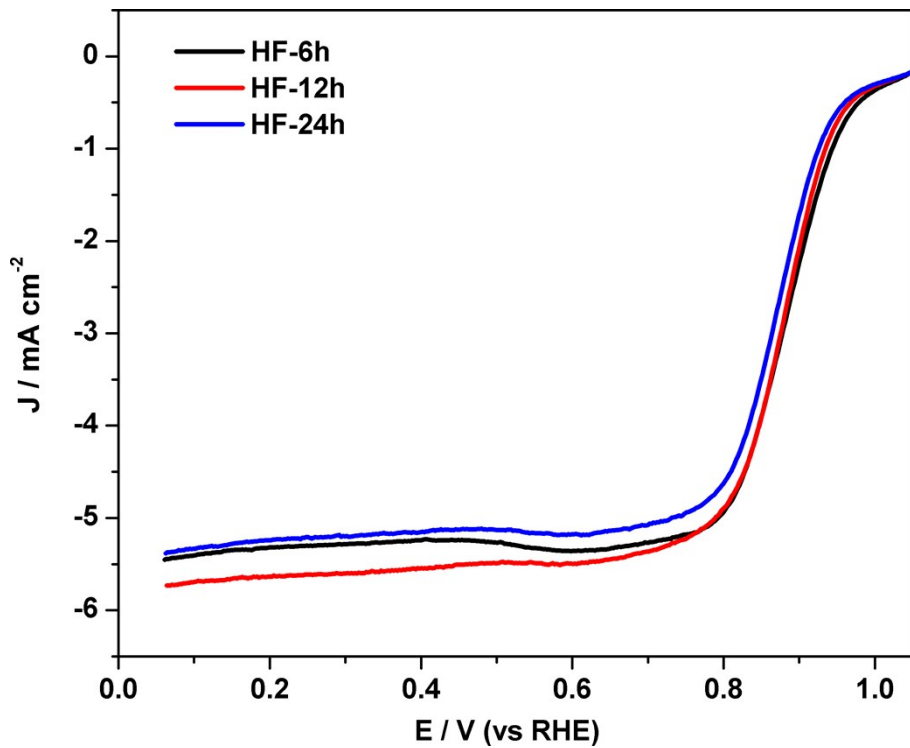


Fig. S15 The ORR LSV plots of Z-CNS-Fe with different etching time.

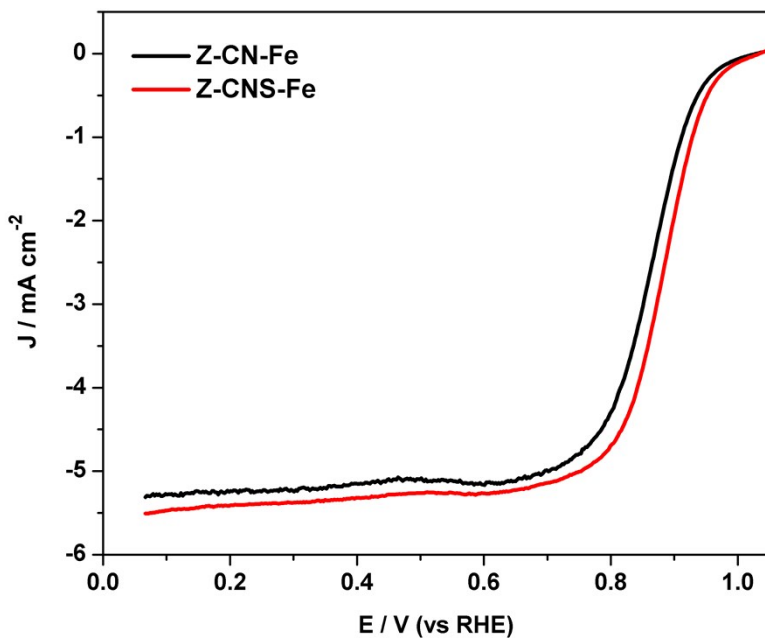


Fig. S16 The ORR LSV plots of Z-CNS-Fe and Z-CN-Fe.

Table S1. The BET surface area and pore properties for the catalysts.

Sample	Surface area ($\text{m}^2 \text{ g}^{-1}$)	Pore volume ($\text{cm}^3 \text{ g}^{-1}$)	Pore size (nm^2)
CNS-Fe	594	0.792	6.61
Z-CNS	1226	1.20	5.75
Z-CNS-Fe-NT	278	0.008	3.08
Z-CNS-Fe	1069	0.214	5.24
Z-CNS-Fe-Dcb	930	0.211	12.99
Z-CNS-Fe-Bpd	983	0.185	7.22

Table S2. The contents of total nitrogen and different types of nitrogen species on the surface of each catalyst from XPS results.

sample	Content of nitrogen species (at%)				Total content (at%)
	Pyridinic-N	Fe-N _x	Pyrrolic-N	Graphitic-N	
Z-CNS-Fe-Dcb	0.974	1.01	0.792	0.824	3.60
Z-CNS-Fe-Bpd	2.49	1.61	1.21	1.29	6.60
Z-CNS-Fe	3.24	2.22	1.37	1.15	7.98

Table S3. The contents of Fe loading from ICP-AES and N content from EA results.

sample	Z-CNS-Fe-Dcb	Z-CNS-Fe-Bpd	Z-CNS-Fe
Fe loading from ICP-AES (wt %)	0.17	0.78	1.04
N content from EA (wt %)	3.67	7.53	7.77

Table S4. Comparison of the ORR activities of Z-CNS-Fe with previously reported Fe-based ORR catalysts.

catalysts	E _{onset} (V)	E _{1/2} (V)	J (mA cm ⁻²)	Loading (μg cm ⁻²)	Ref
Z-CNS-Fe	1.01	0.88	5.52	310	This work
Fe(0)@FeNC	0.95	0.85	6.25	300	1
FeZ-CNS	0.96	0.88	5.63	500	2
Fe-N-C HNSs	1.04	0.87	5.72	255	3
p-Fe-N-CNFs	0.91	0.82	5.10	600	4
FePc/AP-GA	0.96	0.83	5.98	404	5
Fe-N-DSC	1.02	0.83	4.50	100	6
Fe/N/S-CNTs	0.97	0.88	6.00	510	7
S,N-Fe/N/C-CNT	0.97	0.85	6.71	600	8
Fe@BC-800	1.01	0.85	5.34	420	9
Fe-NGM/C-Fe SAC	1.05	0.86	5.70	160	10
MF-Fe-800 SAC	0.98	0.83	4.50	400	11
FeN ₄ -GN	1.05	0.86	3.94	310	12
Fe-N-SCCFs	1.05	0.88	5.64	614	13
Fe ₃ C/NG-800	1.03	0.86	5.98	400	14
PANI-Fe/Silica	0.84	0.73	4.68	100	15

References

1. Z. Li, L. Wei, W.-J. Jiang, Z. Hu, H. Luo, W. Zhao, T. Xu, W. Wu, M. Wu and J.-S. Hu, *Appl. Catal., B*, 2019, **251**, 240-246.
2. G. Li, L. Pei, Y. Wu, B. Zhu, Q. Hu, H. Yang, Q. Zhang, J. Liu and C. He, *J. Mater. Chem. A*, 2019, **7**, 11223-11233.
3. Y. Chen, Z. Li, Y. Zhu, D. Sun, X. Liu, L. Xu and Y. Tang, *Adv. Mater.*, 2019, **31**, 1806312.
4. B.-C. Hu, Z.-Y. Wu, S.-Q. Chu, H.-W. Zhu, H.-W. Liang, J. Zhang and S.-H. Yu, *Energy Environ. Sci.*, 2018, **11**, 2208-2215.
5. J. Huang, Q. Lu, X. Ma and X. Yang, *J. Mater. Chem. A*, 2018, **6**, 18488-18497.
6. Z. Huang, H. Pan, W. Yang, H. Zhou, N. Gao, C. Fu, S. Li, H. Li and Y. Kuang, *ACS Nano*, 2018, **12**, 208-216.
7. H. Jin, H. Zhou, W. Li, Z. Wang, J. Yang, Y. Xiong, D. He, L. Chen and S. Mu, *J. Mater. Chem. A*, 2018, **6**, 20093-20099.
8. P. Chen, T. Zhou, L. Xing, K. Xu, Y. Tong, H. Xie, L. Zhang, W. Yan, W. Chu, C. Wu and Y. Xie, *Angew. Chem., Int. Edition.*, 2017, **56**, 610-614.
9. X. Ma, Z. Lei, W. Feng, Y. Ye and C. Feng, *Carbon*, 2017, **123**, 481-491.
10. C. Wang, H. Zhang, J. Wang, Z. Zhao, J. Wang, Y. Zhang, M. Cheng, H. Zhao and J. Wang, *Chem. Mater.*, 2017, **29**, 9915-9922.
11. B. Lu, T. J. Smart, D. Qin, J. E. Lu, N. Wang, L. Chen, Y. Peng, Y. Ping and S. Chen, *Chem. Mater.*, 2017, **29**, 5617-5628.
12. X. Chen, L. Yu, S. Wang, D. Deng and X. Bao, *Nano Energy*, 2017, **32**, 353-358.
13. B. Wang, X. Wang, J. Zou, Y. Yan, S. Xie, G. Hu, Y. Li and A. Dong, *Nano Letters*, 2017, **17**, 2003-2009.
14. M. Xiao, J. Zhu, L. Feng, C. Liu and W. Xing, *Adv. Mater.*, 2015, **27**, 2521-2527.
15. H.-W. Liang, W. Wei, Z.-S. Wu, X. Feng and K. Müllen, *J. Am. Chem. Soc.*, 2013, **135**, 16002-16005.